J Appl Physiol 104: 212–217, 2008.
First published November 8, 2007; doi:10.1152/japplphysiol.00069.2007.

Gray matter blood flow change is unevenly distributed during moderate isocapnic hypoxia in humans

Andrew P. Binks,[1] Vincent J. Cunningham,[3] Lewis Adams,[4] and Robert B. Banzett[2]

[1]*University of New England, Portland, Maine;* [2]*Harvard Medical School, Boston, Massachusetts;* [3]*Medical Research Council Cyclotron Unit, Imperial College School of Medicine, London, United Kingdom; and* [4]*School of Physiotherapy and Exercise Science, Griffith University, Gold Coast, Queensland, Australia*

Submitted 15 January 2007; accepted in final form 2 November 2007

Binks AP, Cunningham VJ, Adams L, Banzett RB. Gray matter blood flow change is unevenly distributed during moderate isocapnic hypoxia in humans. *J Appl Physiol* 104: 212–217, 2008. First published November 8, 2007; doi:10.1152/japplphysiol.00069.2007.—Hypoxia increases cerebral blood flow (CBF), but it is unknown whether this increase is uniform across all brain regions. We used $H_2{}^{15}O$ positron emission tomography imaging to measure absolute blood flow in 50 regions of interest across the human brain ($n = 5$) during normoxia and moderate hypoxia. P_{CO_2} was kept constant (~44 Torr) throughout the study to avoid decreases in CBF associated with the hypocapnia that normally occurs with hypoxia. Breathing was controlled by mechanical ventilation. During hypoxia (inspired P_{O_2} = 70 Torr), mean end-tidal P_{O_2} fell to 45 ± 6.3 Torr (means ± SD). Mean global CBF increased from normoxic levels of 0.39 ± 0.13 to 0.45 ± 0.13 ml/g during hypoxia. Increases in regional CBF were not uniform and ranged from 9.9 ± 8.6% in the occipital lobe to 28.9 ± 10.3% in the nucleus accumbens. Regions of interest that were better perfused during normoxia generally showed a greater regional CBF response. Phylogenetically older regions of the brain tended to show larger vascular responses to hypoxia than evolutionary younger regions, e.g., the putamen, brain stem, thalamus, caudate nucleus, nucleus accumbens, and pallidum received greater than average increases in blood flow, while cortical regions generally received below average increases. The heterogeneous blood flow distribution during hypoxia may serve to protect regions of the brain with essential homeostatic roles. This may be relevant to conditions such as altitude, breath-hold diving, and obstructive sleep apnea, and may have implications for functional brain imaging studies that involve hypoxia.

stroke; altitude; obstructive sleep apnea

THE GLOBAL RESPONSE OF THE cerebral vasculature to changes in arterial oxygen tension has previously been described (3, 5, 7, 24). Cerebral blood flow (CBF) increases as arterial saturation of oxygen (Sa_{O_2}) falls (5, 7, 23). While there are numerous papers describing the global response of CBF to hypoxia, there is little information on the regional distribution of CBF during hypoxia; the information that does exist is confounded by simultaneous P_{CO_2} changes. We hypothesize that there would be significant differences among brain regions in the blood flow response to hypoxia in the absence of changes in P_{CO_2}.

The most common experimental intervention to produce cerebral hypoxia is exposure to low inspired P_{O_2} without control of other variables. In such experiments, subjects have been allowed to breathe spontaneously during the intervention, and as a consequence the reflex increase in alveolar ventilation also markedly reduced arterial P_{CO_2} (Pa_{CO_2}). Low Pa_{CO_2} reduces CBF, thereby opposing the effect of low P_{O_2} on CBF (10, 38). Outside the laboratory, a similar situation exists at high altitude. In contrast, when cerebral hypoxia is produced by respiratory disease, asphyxia, or ischemia, the P_{CO_2} is generally normal or elevated. Here we held Pa_{CO_2} constant during hypoxia and used $H_2{}^{15}O$ positron emission tomography (PET) to image the CBF response.

It is not known whether the vascular response to hypoxia is uniform across the brain: some evidence suggests that the response to hypoxia is uniform (33); other evidence using autoradiography (45), video microscopy (17), MRI (36), and PET (4, 20) suggests that some brain regions receive a greater CBF increase. Nonuniform flow responses could be important in situations such as altitude and breath-hold diving and in clinical situations such as sleep apnea; more responsive regions may be better protected during these hypoxic episodes.

The present study used $H_2{}^{15}O$ PET to measure regional cerebral blood flow (rCBF) in five healthy men during hypoxia with constant Pa_{CO_2}. The concentration of radioactivity in arterial blood was measured continuously throughout the PET scans to provide an input function that allows quantitative estimates of absolute blood flow to be obtained. We measured rCBF during periods of moderate hypoxia (Sa_{O_2} = 80%) and periods of normoxia (Sa_{O_2} = 97%). Pa_{CO_2} was maintained constant throughout the study by controlling ventilation and inspired P_{CO_2}. Mean regional blood flow responses for 50 functional regions of interest (ROIs) are reported, and the data revealed that there is a nonuniform vascular response to normocapnic hypoxia in humans.

MATERIALS AND METHODS

This study was approved by the Human Subject Committees at Imperial College, London, and at Harvard School of Public Health. Six subjects, all men and all righthanded, gave informed consent. Before the brain imaging study, subjects practiced the protocol in the laboratory so that they were familiar with the procedures, and we could ensure that they were appropriate candidates (i.e., there were no ECG abnormalities during hypoxia). One normal, healthy subject was excluded from the study after cardiac arrhythmias were noted during exposure to hypoxia in a practice session (a normal heart rhythm returned when normoxia was restored). We were unable to replace the excluded subject due to logistical constraints.

Physiological measurements. Tidal volume (V_T) and respiratory frequency were controlled by mechanical ventilation (Siemens 900B in volume control mode) via a mouthpiece at an initial minute

Address for reprint requests and other correspondence: A. P. Binks, Dept. of Health Sciences, Univ. of New England, 716 Stevens Ave., Portland, ME (e-mail: abinks@une.edu).

The costs of publication of this article were defrayed in part by the payment of page charges. The article must therefore be hereby marked "*advertisement*" in accordance with 18 U.S.C. Section 1734 solely to indicate this fact.

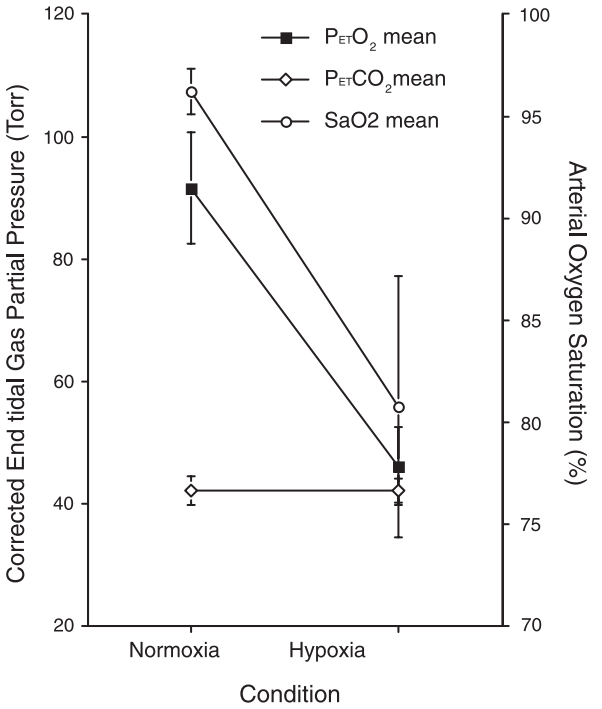

Fig. 1. Mean ± SD end-tidal gas pressures (O_2 and CO_2) and arterial saturation during normoxia and hypoxia. $P_{ET_{O_2}}$, end-tidal P_{O_2}; $P_{ET_{CO_2}}$, end-tidal P_{CO_2}; Sa_{O_2}, arterial O_2 saturation.

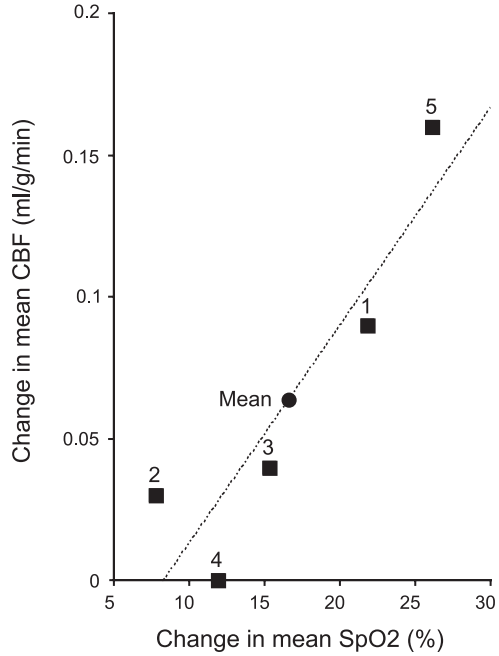

Fig. 2. Changes in mean global cerebral blood flow (CBF) for each subject (■, subject number shown) and group mean (●) with changes in arterial saturation. Dashed line is a linear regression ($r^2 = 0.82$). Sp_{O_2}, Sa_{O_2} from pulse oximetry.

ventilation approximate to 0.16 l·min^{-1}·kg body wt^{-1}, and a respiratory rate of 12 breaths/min. Airway pressure, VT, and respiratory frequency were recorded from the analog output of the ventilator. Heart rate and Sa_{O_2} were measured from the index finger using a pulse oximeter (Sp_{O_2}) (Biox 3700, Ohmeda, Louisville, CO). Because hypoxia poses a cardiac risk, subjects were monitored using a 12-lead ECG; for safety, maximal hypoxia was limited to Sp_{O_2} not less than 70%. End-tidal P_{CO_2} ($P_{ET_{CO_2}}$) and P_{O_2} ($P_{ET_{O_2}}$) were measured at the mouth (Capnograph, PK Morgan, Haverhill, MA; LB1, Liston Scientific, Irvine, CA, respectively) and corrected to give estimates of arterial levels (22).

PET measurements. PET scans were carried out on a CTI 966 PET scanner (Siemens, Oxford, UK) with a 24-cm-deep field of view. The field of view was positioned to include the whole brain, including cerebellum and brain stem. The mean spatial resolution was 4.8 ± 0.2 mm (transaxial, 1 cm off-axis) and 5.6 ± 0.5 mm (axial, on-axis).

Each subject underwent 15 scans (3 sessions of 5 scans, see below) following a bolus intravenous injection of $H_2{}^{15}O$ (0.5 mSi/scan). The concentration of $H_2{}^{15}O$ was measured continuously in arterial blood drawn from the radial artery throughout each scan (41).

Protocol. There were three interventions made: *1*) normoxia with baseline VT (mean = 0.86 ± 0.12 liter); this intervention produced no dyspnea; *2*) hypoxia with baseline VT (mean = 0.89 ± 0.11 liter); although this intervention was intended to cause dyspnea, it was not consistently effective; and *3*) hypoxia with large VT (mean = 1.43 ± 0.13 liter); this condition produced no dyspnea. Each intervention was 8 min long, and an imaging session (5 images) consisted of one of each type presented in a randomized order. Data for this report were generated during a study that was partially designed to investigate the neural activations associated with dyspnea caused by hypoxia. The dyspnea study was not published, because the intervention intended to cause dyspnea failed to cause adequate dyspnea within the hypoxia safety limit. This did not affect our second objective, because the level of hypoxia achieved did produce significant increases in CBF.

During the hypoxia interventions, inspired oxygen was reduced from 20 to 10% (inspired P_{O_2} = 70 Torr), which reduced Sp_{O_2} to a mean value of ~80%. This level of hypoxia is expected to induce a substantial vascular response [threshold for vascular response is 90% (14)]. To avoid changes in CBF associated with changes in Pa_{CO_2}, we maintained $P_{ET_{CO_2}}$ constant. VT, frequency, and inspired CO_2 fraction ($F_{I_{CO_2}}$) were the same during *conditions 1* and *2*; thus alveolar ventilation and $P_{ET_{CO_2}}$ did not differ. *Condition 3* employed a higher VT; thus we increased $F_{I_{CO_2}}$ to keep $P_{ET_{CO_2}}$ constant in the face of increased alveolar ventilation. In all conditions, continual fine tuning of $F_{I_{CO_2}}$ was done by an experimenter using feedback from the capnometer trace to keep $P_{ET_{CO_2}}$ at the desired value (9).

Table 1. *Physiological data for each subject during hypoxia and normoxia*

	Sa_{O_2}, %		$P_{ET_{O_2}}$, Torr		$P_{ET_{CO_2}}$, Torr		Whole Brain Blood Flow, ml·g^{-1}·min^{-1}	
Subject No.	Hypoxia	Normoxia	Hypoxia	Normoxia	Hypoxia	Normoxia	Hypoxia	Normoxia
1	75.2±3.9	97.0±1.0	44.0±2.8	98.0±3.5	42.1±1.0	42.6±1.3	0.48±0.08	0.39±0.12
2	88.8±1.8	96.6±0.5	54.6±5.2	93.0±0.7	42.1±0.3	41.8±0.4	0.40±0.07	0.37±0.02
3	80.9±2.5	96.2±0.4	40.2±2.1	85.0±0.7	44.3±0.7	43.8±0.8	0.51±0.05	0.47±0.10
4	84.5±4.6	96.4±0.9	46.7±5.5	96.0±2.8	45.1±0.7	45.4±0.5	0.40±0.07	0.40±0.03
5	70.6±4.0	96.6±0.9	41.9±2.4	94.0±1.6	43.9±0.7	44.2±1.5	0.62±0.20	0.46±0.10

Values are means ± SD. Sa_{O_2}, arterial O_2 saturation; $P_{ET_{O_2}}$, end-tidal P_{O_2}; $P_{ET_{CO_2}}$, end-tidal P_{CO_2}.

Signal processing. Quantitative functional images of rCBF were generated as described by Lammertsma et al. (26) using the integrated tissue radioactivity from 30 to 120 s after scan start. The time delay associated with the blood counter was measured by comparison of the blood time activity curve with that of the total count rate of the scanner. A lookup table relating the expected integral tissue activity to blood flow rate was then generated, assuming a dispersion effect in the measured blood with a time constant of 8 s, together with an equilibrium partition coefficient for $H_2{}^{15}O$ of 0.86 ml blood/ml brain tissue. The lookup table was then used to convert the integral images to quantitative CBF images on a pixel-by-pixel basis.

Flow images were placed into standard brain space [Montreal Neurological Institute Space (12); Statistical Parametric Mapping 99 (SPM99; Wellcome Dept. of Cognitive Neurology, Institute of Neurology, London; http://www.fil.ion.ucl.ac.uk/spm)]. Images were then spatially smoothed (4 mm full-width half-maximum). Because inclusion of CSF or white matter in any of the brain volumes would likely cause an underestimation of blood flow, white matter and CSF were masked out. To do this, we removed areas with a signal $< 80\%$ of the mean signal (SPM99) before further analysis was performed. The remaining gray matter images were then divided into 50 ROI using in-house software (Marsbar, SPM99) (15). (See Table 2 for the ROI designations.) Absolute mean blood flow was calculated for each ROI for periods of hypoxia and normoxia.

Periods of hypoxia were compared with periods of normoxia for each subject and for the group; the absolute and relative (percentage) differences in blood flow were calculated for each ROI. *Interventions 2* and *3* were grouped as the hypoxia condition (as there was no significant difference between the flow changes seen in these interventions, analysis of covariance). *Intervention 1* was the normoxia intervention. All values are means ± SD.

RESULTS

Physiological interventions. Reduction in inspired O_2 levels caused $P_{ET_{O_2}}$ to fall significantly ($P < 0.05$) from 93.8 ± 4.8

Table 2. *Designated ROI for comparison of normoxic and hypoxic blood*

ROI	Phylogenetic Age	Normoxic CBF, ml·g^{-1}·min^{-1}	Hypoxic ΔCBF, ml·g^{-1}·min^{-1}	Hypoxic ΔCBF, %
Occipital lobe, right	New	0.414±0.033	0.040±0.034*	9.9±8.6
Anterior temporal lobe, right	New	0.423±0.050	0.041±0.046	10.2±11.1
Gyrus cinguli, anterior, left	New	0.431±0.028	0.044±0.042*	10.3±10.0
Anterior temporal lobe, lateral, left	New	0.330±0.047	0.040±0.042	10.8±10.7
Anterior temporal lobe, lateral, right	New	0.337±0.045	0.036±0.036*	11.1±10.7
Lateral occipitotemporal gyrus right	New	0.351±0.028	0.038±0.033*	11.1±9.7
Frontal lobe, left	New	0.550±0.058	0.061±0.046*	11.3±8.8
Parahippocampal, right	Old	0.330±0.030	0.037±0.035*	11.7±10.9
Gyrus cinguli, anterior part, right	New	0.431±0.028	0.061±0.054*	12.0±10.7
Middle and inferior temporal gyri, left	New	0.443±0.035	0.043±0.036*	12.1±9.7
Posterior temporal lobe, right	New	0.366±0.030	0.044±0.036*	12.2±10.1
Middle and inferior temporal gyri, right	New	0.433±0.035	0.054±0.042*	12.5±10.0
Parietal lobe , left	New	0.376±0.026	0.047±0.037*	12.5±9.8
Parietal lobe, right	New	0.373±0.024	0.046±0.036*	12.7±10.2
Superior temporal gyrus, left	New	0.469±0.038	0.061±0.045*	12.8±9.2
Caudate nucleus, left	Old	0.392±0.022	0.050±0.039*	12.8±9.9
Cerebellum, right	Old	0.312±0.021	0.040±0.040*	13.0±12.5
Anterior temporal lobe, medial, left	New	0.330±0.047	0.041±0.038*	13.1±12.6
Gyrus cinguli, posterior part, right	New	0.514±0.049	0.066±0.039*	13.1±8.3
Parahippocampal, left	Old	0.385±0.039	0.049±0.036*	13.2±10.1
Superior temporal gyrus, right	New	0.388±0.040	0.050±0.044*	13.3±11.9
Lateral occipitotemporal gyrus, left	New	0.324±0.024	0.043±0.031*	13.6±10.3
Frontal lobe, right	New	0.393±0.031	0.052±0.041*	13.7±10.7
Posterior temporal lobe, left	New	0.412±0.027	0.057±0.043*	14.0±10.3
Amygdala, left	Old	0.417±0.048	0.057±0.041*	14.4±10.4
Insula, right	Old	0.443±0.042	0.067±0.051*	14.8±10.3
Cerebellum, left	Old	0.407±0.035	0.062±0.043*	15.1±10.3
Gyrus cinguli, posterior, left	Old	0.588±0.059	0.088±0.047*	15.3±8.6
Whole brain		0.417±0.043	0.066±0.066*	15.5±14.7
Occipital lobe left	New	0.434±0.022	0.069±0.047*	15.8±10.6
Brain stem	Old	0.412±0.028	0.065±0.043*	15.8±10.4
Hippocampus, right	Old	0.063±0.007	0.010±0.007*	15.9±12.1
Hippocampus, left	Old	0.401±0.033	0.066±0.045*	17.0±12.4
Insula left	Old	0.363±0.032	0.063±0.038*	17.1±9.9
Thalamus right	Old	0.460±0.042	0.080±0.043*	17.5±9.2
Nucleus accumbens left	Old	0.338±0.042	0.058±0.033*	17.7±9.9
Putamen, right	Old	0.515±0.032	0.093±0.056*	17.9±10.3
Amygdala, right	Old	0.396±0.027	0.070±0.054*	18.0±14.2
Pallidum right	Old	0.419±0.041	0.078±0.045*	18.5±9.7
Caudate nucleus right	Old	0.354±0.035	0.064±0.040*	18.6±11.8
Thalamus, left	Old	0.522±0.031	0.097±0.057*	18.9±11.4
Pallidum, left	Old	0.478±0.039	0.092±0.055*	19.3±11.2
Putamen, left	Old	0.468±0.015	0.091±0.062*	19.7±13.7
Nucleus accumbens, right	Old	0.354±0.035	0.125±0.040*	28.9±10.3

Values are asolute mean ± SD (in ml·g^{-1}·min^{-1}) and percent mean changes in regional blood flow. Regions of interest (ROIs) are listed in ascending order of blood flow response. Each ROI has been labeled as either phylogenetically "old" or "new" (28). The absolute blood flow during normoxia is given. CBF, cerebral blood flow. Δ, change. *Significant change (*t*-test, $P < 0.05$) in regional CBF from normoxia to hypoxia. Two regions did not show a significant change: the medial part of the right anterior temporal lobe (*t*-test, $P = 0.16$) and the lateral part of the left anterior temporal lobe (*t*-test, $P = 0.25$).

to 45.5 ± 6.3 Torr. $SpSp_{O_2}$ fell from 96.6 ± 0.8 to 80.0 ± 7.4%. There was a wide range in the saturation change induced: from 7.8% (*subject 2*) to 26.1% (*subject 5*). The difference in $P_{ET}CO_2$ between hypoxic and normoxic conditions was calculated for each subject (range, −0.5 to 0.5 Torr). The group mean change in $P_{ET}CO_2$ between the two conditions was 0.06 ± 0.43 Torr (*T*-test, $P = 0.77$). The absolute mean values for $P_{ET}CO_2$ were 43.6 ± 1.5 Torr during normoxia and 43.5 ± 1.4 Torr during hypoxia. Arterial saturation and end-tidal gas data are shown in Fig. 1. Physiological data for each subject are shown in Table 1.

Changes in CBF. Whole brain measurements showed that hypoxia significantly increased global CBF (gCBF) in four of the five subjects. Mean gCBF was 0.39 ± 0.10 $ml \cdot g^{-1} \cdot min^{-1}$ during normoxia and significantly increased (*T*-test, $P < 0.05$) to 0.45 ± 0.13 $ml \cdot g^{-1} \cdot min^{-1}$ during hypoxia (a 14.8% rise above normoxic levels). In general, the magnitude of the gCBF response was correlated with the level of desaturation induced ($r^2 = 0.82$, linear regression; see Fig. 2).

The magnitude of the hypoxia-driven blood flow increase to an ROI was significantly related to the ROI's normoxic blood flow (ANOVA, $P < 0.05$), i.e., the greater the blood flow during normoxia, the greater the hypoxic response. Relative increases in gray matter blood flow were not uniform across the specified ROI. Increases ranged from only 0.04 $ml \cdot g^{-1} \cdot min^{-1}$ (9% increase) in the right occipital lobe to 0.12 $ml \cdot g^{-1} \cdot min^{-1}$ (28.9% increase) in the right nucleus accumbens. There was a trend for phylogenically "older" parts of the brain to receive both a greater absolute blood flow and a greater increase in blood flow. For example, the nuclei of the basal ganglia showed consistently higher increases in blood flow during hypoxia than most other brain regions (putamen, 19.7 ± 13.6%; pallidum, 18.5 ± 9.7%; caudate nucleus, 18.6 ± 11.8%), while the cerebral hemispheres generally received a smaller increase in blood flow (e.g., frontal lobe, 11.3 ± 8.8%; temporal lobe, 10.2 ± 11.1%; parietal lobe, 12.2 ± 10.1%). The absolute and relative changes in blood flow are shown for each ROI in Table 2. After designating each ROI as either "old" (archipallium and palleomammalian brain) or "new" (neopallium brain) (Ref. 28; see Table 2), we determined that blood flow response of old regions (16.9 ± 3.6%) was significantly greater (Wilcoxon test, $P < 0.05$) than the response of new regions (13.23 ± 2.6%). A summary of the rCBF changes for old and new brain is shown in Fig. 3.

The pattern of blood flow distribution was not significantly different among subjects (analysis of covariance, $P = 0.34$): this included *subject 4*, who, despite not showing a significant whole brain response, did show the same pattern of changes in the individual ROI as the other subjects.

DISCUSSION

We found that the increase in CBF during isocapnic hypoxia was not uniform: a number of brain regions received a proportionally greater increase in blood flow. The most prominent increases in blood flow were seen in the nuclei of the basal ganglia, as well as several other phylogenetically old brain regions, specifically the putamen, the thalamus, nucleus accumbens, and the pallidum.

Our study has confirmed previous findings, as well as shown new information. The gCBF increase (14.8%) observed at this level of hypoxia (Sp_{O_2} = 80.0 ± 7.4%) is similar to increases seen in previous studies (4, 30, 37). The present investigation, however, has determined blood flow changes more focused and numerous ROIs. The two earlier studies that measured rCBF during hypoxia used an intervention that produced both hypoxia and hypocapnia. Buck et al. (4) showed only a small decrease in P_{CO_2} during hypoxia (1.5 Torr), but this may have been sufficient to cause a 3–4% change in CBF. However, we also note that the subjects in the study of Buck et al. started with relatively low P_{CO_2}, (36 Torr), and so hypoxia periods may have included a hypocapnic contribution to blood flow changes. Hypocapnia reduces gCBF (11, 20, 37, 40) and may have attenuated regional inhomogeneity. Nonetheless, these two studies detected relative increases in two of the regions we observed: basal ganglia (33) and thalamus (4).

The areas that received a proportionally greater blood flow during hypoxia are mostly perfused by the lenticulostriate arteries [branches of the middle cerebral artery (MCA)]. The

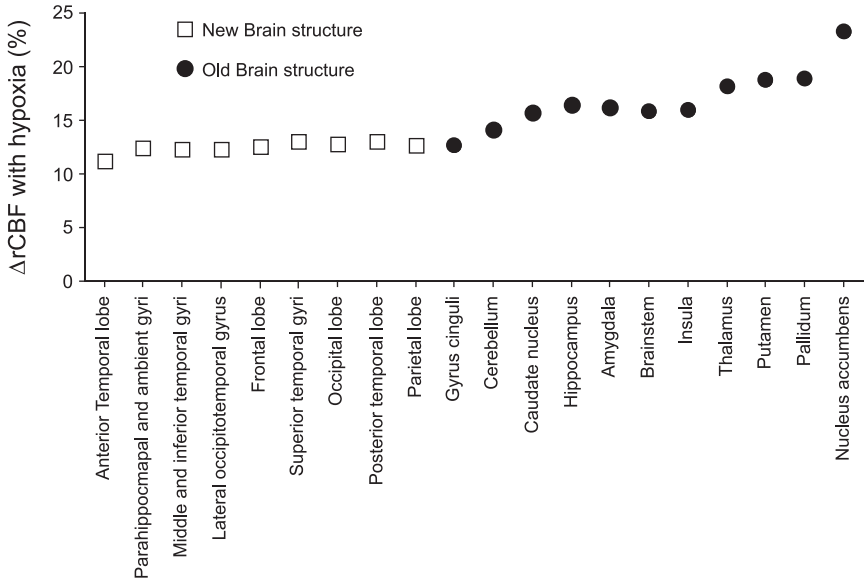

Fig. 3. Changes in CBF to different regions of interest during hypoxia. Structures are listed in ascending order of blood flow increase. For clarity, region of interest data shown are the mean of the left and right side of the brain (full details in Table 2). Changes in regional CBF (ΔrCBF) are expressed as a percent increase above normoxic levels. □, New brain structures; ●, old brain structures.

responses of the main trunk of the MCA to hypercapnia (19), hypoxia (37, 39), and hyperoxia (44) have been extensively described, perhaps because of its accessibility to Doppler ultrasound, but no Doppler studies have compared the hypoxic responses of different cerebral vessels. It is unclear whether the MCA or the lenticulostriate arteries have a greater sensitivity to hypoxia than other cerebral vessels. Doppler evidence from the hypoxic human fetal brain suggests that the anterior cerebral artery has a more sustained vasodilation to chronic hypoxia than either the MCAs or posterior cerebral arteries (6), affording the frontal lobes of the fetal brain better protection than the "primitive brain" regions we have described in the adult brain. However, the fetal cerebrovasculature shows a different response to hypercapnia than the adult (18) and may show a different response to acute hypoxia, as used in this study. The response of the rat brain shows similar blood flow distributions to those we observed during hypoxic-ischemia, with the cerebral cortex receiving less protection than other brain regions (43) and hypoxic hypercapnia results in thalamic regions of the piglet brain being better perfused than the cerebral cortex (1). From this and previous studies, it appears that some brain regions are afforded better protection against hypoxia than others.

The cerebrovascular response protects the brain against hypoxia during conditions such as obstructive sleep apnea, suffocation, and drowning (situations in which there is no concurrent fall in P_{CO_2}, as during exposure to hypobaria). The nucleus accumbens had the greatest perfusion increase in our study, and this area has been shown to suffer less anoxic damage than other brain regions in humans (16) and in piglets (29). The mechanism by which certain regions of the brain are better protected from arterial gas changes is not clear, but may be related to the present findings. Ito et al. (20) also saw the "older" brain (pons, cerebellum, thalamus, and putamen) receiving proportionally greater increases in blood flow during hypercapnia than the frontal, temporal, occipital, and parietal cortexes. Hypoxia and hypercapnia-induced changes in CBF may share common mediators and/or pathways, although an obvious candidate, the peripheral chemoreceptor, does not appear to be involved with CBF control (31). Regional changes in pH can also influence local blood flow during both hypercapnia (25) and hypoxia (27). Hypoxic and hypercapnic changes in vascular tone may both be mediated by adenosine (35) or nitric oxide (34), although the direct role of the latter is less clear (13). The highest concentrations of the A_2 adenosine receptor (that are thought to be involved with vascular tone) are found in the caudate, putamen, and nucleus accumbens (21): three regions receiving high blood flow during hypoxia. The regional distribution of the enzyme nitric oxide synthase in the rat (34) or human brain (2) does not seem to correlate with the distribution of blood flow seen in this study.

Preservations of the older brain regions responsible for homeostatic function (32) may have provided a selective advantage. When sudden and complete anemia is induced in the cat, the survival time of cerebral structures appears related to the regional blood flow measurements seen in this study, with older structures surviving 25–40 s and the cerebral cortex lasting only 14–15 s (42).

The heterogeneity of blood flow distribution during hypoxia complicates studies that use blood flow distribution as an indicator of brain function, e.g., functional MRI and $H_2{}^{15}O$ PET. Without compensating for the vascular changes associated with hypoxia per se, redistribution of blood flow could easily be misinterpreted as increases in local neural activity. Changes in arterial CO_2 also present a similar problem (46), and, because Pa_{CO_2} is more easily influenced by changes in breathing than $SpSp_{O_2}$, extra precautions should be taken.

In summary, the changes in blood flow associated with hypoxia are not equally distributed across the brain. In general, greater flow is directed to the older brain (e.g., nucleus accumbens, putamen, pallidum, caudate, thalamus), possibly to maintain essential homeostatic functions, even at the cost of reduced cognitive function. This heterogeneity should be acknowledged and accounted for during functional brain imaging studies where hypoxia may be present.

ACKNOWLEDGMENTS

Our sincere thanks go to the subjects who participated in the study. We acknowledge the invaluable contribution of Andrew Blythe, Jasbir Grewal, and the staff at the Hammersmith Cyclotron Unit. Kevin Murphy of Charing Cross Hospital, London, provided superb support for this study, as well as Karl Evans and Claudine Peiffer, who assisted in the original study from which these data were derived.

GRANTS

This research was supported by National Heart, Lung, and Blood Institute grant HL46690, The Breathlessness Charitable Trust, and the Medical Research Council.

REFERENCES

1. **Bauer R, Bergmann R, Walter B, Brust P, Zwiener U, Johannsen B.** Regional distribution of cerebral blood volume and cerebral blood flow in newborn piglets–effect of hypoxia/hypercapnia. *Brain Res Dev Brain Res* 112: 89–98, 1999.
2. **Blum-Degen D, Heinemann T, Lan J, Pedersen V, Leblhuber F, Paulus W, Riederer P, Gerlach M.** Characterization and regional distribution of nitric oxide synthase in the human brain during normal ageing. *Brain Res* 834: 128–135, 1999.
3. **Borgstrom L, Johannsson H, Siesjo BK.** The relationship between arterial P_{O_2} and cerebral blood flow in hypoxic hypoxia. *Acta Physiol Scand* 93: 423–432, 1975.
4. **Buck A, Schirlo C, Jasinksy V, Weber B, Burger C, von Schulthess GK, Koller EA, Pavlicek V.** Changes of cerebral blood flow during short-term exposure to normobaric hypoxia. *J Cereb Blood Flow Metab* 18: 906–910, 1998.
5. **Cohen PJ, Alexander SC, Smith TC, Reivich M, Wollman H.** Effects of hypoxia and normocarbia on cerebral blood flow and metabolism in conscious man. *J Appl Physiol* 23: 183–189, 1967.
6. **Dubiel M, Gunnarsson GO, Gudmundsson S.** Blood redistribution in the fetal brain during chronic hypoxia. *Ultrasound Obstet Gynecol* 20: 117–121, 2002.
7. **Ellingsen I, Hauge A, Nicolaysen G, Thoresen M, Walloe L.** Changes in human cerebral blood flow due to step changes in PAO2 and PACO2. *Acta Physiol Scand* 129: 157–163, 1987.
8. **Evans KC, Banzett RB, Adams L, McKay L, Frackowiak RS, Corfield DR.** BOLD fMRI identifies limbic, paralimbic, and cerebellar activation during air hunger. *J Neurophysiol* 88: 1500–1511, 2002.
9. **Fortune JB, Bock D, Kupinski AM, Stratton HH, Shah DM, Feustel PJ.** Human cerebrovascular response to oxygen and carbon dioxide as determined by internal carotid artery duplex scanning. *J Trauma* 32: 618–627, 1992.
10. **Fortune JB, Feustel PJ, deLuna C, Graca L, Hasselbarth J, Kupinski AM.** Cerebral blood flow and blood volume in response to O_2 and CO_2 changes in normal humans. *J Trauma* 39: 463–471, 1995.
11. **Friston K, Ashburner J, Poline J, Frith C, Heather J, Frackowiak R.** Spatial registration and normalisation of images. *Hum Brain Mapp* 2: 165–189, 1995.
12. **Goadsby PJ.** Nitric oxide is not the sole determinant of hypercapnic or metabolically driven vasodilation in the cerebral circulation. *J Auton Nerv Syst* 49, *Suppl*: S67–S72, 1994.

14. **Gupta AK, Menon DK, Czosnyka M, Smielewski P, Jones JG.** Thresholds for hypoxic cerebral vasodilation in volunteers. *Anesth Analg* 85: 817–820, 1997.
15. **Hammers A, Koepp MJ, Free SL, Brett M, Richardson MP, Labbe C, Cunningham VJ, Brooks DJ, Duncan J.** Implementation and application of a brain template for multiple volumes of interest. *Hum Brain Mapp* 15: 165–174, 2002.
16. **Huang KW, Zhao Y.** Selective sparing of human nucleus accumbens in aging and anoxia. *Can J Neurol Sci* 22: 290–293, 1995.
17. **Hudetz AG, Biswal BB, Feher G, Kampine JP.** Effects of hypoxia and hypercapnia on capillary flow velocity in the rat cerebral cortex. *Microvasc Res* 54: 35–42, 1997.
18. **Hurn PD, Traystman RJ.** Changes in arterial gas tension. In: *Cerebral Blood Flow and Metabolism* (2nd Ed.), edited by Edvinsson L and Krause DN. Philidelphia, PA: Lippincott Williams and Wilkins, 2002, p. 385–394.
19. **Ide K, Eliasziw M, Poulin MJ.** Relationship between middle cerebral artery blood velocity and end-tidal P_{CO_2} in the hypocapnic-hypercapnic range in humans. *J Appl Physiol* 95: 129–137, 2003.
20. **Ito H, Yokoyama I, Iida H, Kinoshita T, Hatazawa J, Shimosegawa E, Okudera T, Kanno I.** Regional differences in cerebral vascular response to Pa_{CO_2} changes in humans measured by positron emission tomography. *J Cereb Blood Flow Metab* 20: 1264–1270, 2000.
21. **Jarvis MF, Williams M.** Direct autoradiographic localization of adenosine A2 receptors in the rat brain using the A2-selective agonist, [3H]CGS 21680. *Eur J Pharmacol* 168: 243–246, 1989.
22. **Jones NL, Robertson DG, Kane JW.** Difference between end-tidal and arterial P_{CO_2} in exercise. *J Appl Physiol* 47: 954–960, 1979.
23. **Kety S, Schmidt C.** The effects of altered arterial tensions of carbon dioxide and oxygen on cerebral blood flow and cerebral oxygen consumption of normal young men. *J Clin Invest* 27: 484–492, 1948.
24. **Kolb JC, Ainslie PN, Ide K, Poulin MJ.** Protocol to measure acute cerebrovascular and ventilatory responses to isocapnic hypoxia in humans. *Respir Physiol Neurobiol* 141: 191–199, 2004.
25. **Kuschinsky W, Suda S, Sokoloff L.** Local cerebral glucose utilization and blood flow during metabolic acidosis. *Am J Physiol Heart Circ Physiol* 241: H772–H777, 1981.
26. **Lammertsma AA, Cunningham VJ, Deiber MP, Heather JD, Bloomfield PM, Nutt J, Frackowiak RS, Jones T.** Combination of dynamic and integral methods for generating reproducible functional CBF images. *J Cereb Blood Flow Metab* 10: 675–686, 1990.
27. **Lockwood AH, Peek KE, Izumiyama M, Yap EW, Labove J.** Effects of moderate hypoxemia and unilateral carotid ligation on cerebral glucose metabolism and acid-base balance in the rat. *J Cereb Blood Flow Metab* 9: 342–349, 1989.
28. **MacLean PD.** *The Triune Brain in Evolution: Role in Paleocerebral Functions*. New York: Plenum, 1990.
29. **Martin LJ, Brambrink A, Koehler RC, Traystman RJ.** Primary sensory and forebrain motor systems in the newborn brain are preferentially damaged by hypoxia-ischemia. *J Comp Neurol* 377: 262–285, 1997.
30. **Meadows GE, O'Driscoll DM, Simonds AK, Morrell MJ, Corfield DR.** Cerebral blood flow response to isocapnic hypoxia during slow-wave sleep and wakefulness. *J Appl Physiol* 97: 1343–1348, 2004.
31. **Miyabe M, Jones MD Jr, Koehler RC, Traystman RJ.** Chemodenervation does not alter cerebrovascular response to hypoxic hypoxia. *Am J Physiol Heart Circ Physiol* 257: H1413–H1418, 1989.
32. **Noble J, Jones JG, Davis EJ.** Cognitive function during moderate hypoxaemia. *Anaesth Intensive Care* 21: 180–184, 1993.
33. **Pagani M, Ansjon R, Lind F, Uusijarvi J, Sumen G, Jonsson C, Salmaso D, Jacobsson H, Larsson SA.** Effects of acute hypobaric hypoxia on regional cerebral blood flow distribution: a single photon emission computed tomography study in humans. *Acta Physiol Scand* 168: 377–383, 2000.
34. **Pelligrino DA, Koenig HM, Albrecht RF.** Nitric oxide synthesis and regional cerebral blood flow responses to hypercapnia and hypoxia in the rat. *J Cereb Blood Flow Metab* 13: 80–87, 1993.
35. **Phillis JW.** Adenosine and adenine nucleotides as regulators of cerebral blood flow: roles of acidosis, cell swelling, and KATP channels. *Crit Rev Neurobiol* 16: 237–270, 2004.
36. **Posse S, Olthoff U, Weckesser M, Jancke L, Muller-Gartner HW, Dager SR.** Regional dynamic signal changes during controlled hyperventilation assessed with blood oxygen level-dependent functional MR imaging. *AJNR Am J Neuroradiol* 18: 1763–1770, 1997.
37. **Poulin MJ, Liang PJ, Robbins PA.** Dynamics of the cerebral blood flow response to step changes in end-tidal P_{CO_2} and P_{O_2} in humans. *J Appl Physiol* 81: 1084–1095, 1996.
38. **Poulin MJ, Liang PJ, Robbins PA.** Fast and slow components of cerebral blood flow response to step decreases in end-tidal P_{CO_2} in humans. *J Appl Physiol* 85: 388–397, 1998.
39. **Poulin MJ, Robbins PA.** Changes in blood flow in the middle cerebral artery in response to acute isocapnic hypoxia in humans. *Adv Exp Med Biol* 393: 287–292, 1995.
40. **Ramsay SC, Murphy K, Shea SA, Friston KJ, Lammertsma AA, Clark JC, Adams L, Guz A, Frackowiak RS.** Changes in global cerebral blood flow in humans: effect on regional cerebral blood flow during a neural activation task. *J Physiol* 471: 521–534, 1993.
41. **Ranicar A, Williams C, Schnorr L, Clark J, Rhodes C, Bloomfield PM, Jones T.** The online monitoring of continuously withdrawn arterial blood during PET studies using a single BG/photomultiplier assembly and non-stick tubing. *Med Prog Technol* 17: 259–264, 1991.
42. **Sugar O, Gerard RW.** Anoxia and brain potentials. *J Neurophysiol* 1: 558–572, 1938.
43. **Vannucci RC, Lyons DT, Vasta F.** Regional cerebral blood flow during hypoxia-ischemia in immature rats. *Stroke* 19: 245–250, 1988.
44. **Vovk A, Cunningham DA, Kowalchuk JM, Paterson DH, Duffin J.** Cerebral blood flow responses to changes in oxygen and carbon dioxide in humans. *Can J Physiol Pharmacol* 80: 819–827, 2002.
45. **Weiss HR, Buchweitz-Milton E.** Role of alpha-adrenoceptors in the control of the cerebral blood flow response to hypoxia. *Eur J Pharmacol* 148: 107–113, 1988.
46. **Wise RG, Ide K, Poulin MJ, Tracey I.** Resting fluctuations in arterial carbon dioxide induce significant low frequency variations in BOLD signal. *Neuroimage* 21: 1652–1664, 2004.